SYNTHESIS, PURIFICATION, SOLUBILITY, AND RAMAN SPECTROSCOPY STUDY OF VARIOUS SEGMENTS OF THE PROTEIN α-SYNUCLEIN'S NONAMYLOID-BETA COMPONENT REGION

By

Ashton M. Stowe

A Thesis Submitted in Partial Fulfillment

of the Requirements for the Degree of

Master of Science in Chemistry

Middle Tennessee State University

August 2021

Thesis Committee:

Dr. Chengshan Wang

Dr. Ngee Sing Chong

Dr. Kevin Bicker

ACKNOWLEDGEMENTS

I would like to thank my research advisor Dr. Chengshan Wang for his guidance and support throughout my thesis research experience. I would also like to send a sincere thank you to the other members of my thesis committee Dr. Kevin Bicker and Dr. Ngee Sing Chong for their assistance in the lab and for their time spent reviewing and providing valuable suggestions towards my thesis work.

I want to especially thank the MTSU College of Basic and Applied Sciences and the College of Graduate studies for hiring me as a graduate teaching assistant and providing me the opportunity to pursue my masters. The MTSU chemistry department has been very supportive and hands on in aiding my career goals and providing supportive resources to carry out my chemistry research.

I would also like to thank Jessie Weatherly for his constant assistance with our instrumentation and for answering or looking into any and all questions I may have had. I want to thank my peers in the department that helped me in any way during my master's experience.

Finally, I would like to thank my father, Chip Stowe and my grandmother, Louise Stowe, from the bottom of my heart for their endless support, love, and encouragement throughout this journey.

ABSTRACT

Parkinson's Disease is a neurodegenerative brain disorder that occurs when dopamine producing neurons, in the mid-region of the brain known as the substantia nigra, stop working or die. The degenerating dopaminergic neurons develop a hallmark deposition of Lewy bodies comprised mostly of a 140 amino acid residue protein known as α-synuclein. The primary structure of α-synuclein consists of three components: 1) the N-terminus domain (amino acid residues 1-60), which contains a positively charged lysine residue; 2) the hydrophobic domain (residues 61-95), which is the central part of the protein, and is known as the nonamyloid-beta component (NAC); 3) the C-terminus domain (residues 96-140), which is negatively charged and rich in acidic residues.

It has been determined that the NAC is hydrophobic and known to be the source of aggregation within α-synuclein that causes Parkinson's Disease. Previously published results from our lab determined that the NAC shares similar biophysical behavior to that of the whole protein of α-synuclein. On the other hand, it was very insoluble and had weak Raman spectroscopic peaks. For this thesis, the goal was to try to improve the solubility of the NAC region by synthesizing shorter and longer length nonamyloid-beta component (NAC) regions of α-synuclein, observe which are more soluble in water, and analyze each pure peptide using Raman spectroscopy in order to determine if any displayed stronger signals than that of the NAC. It was concluded that all studied variations of the NAC had much greater solubility, but α-synuclein (57-102) had substantially improved Raman spectra signals.

TABLE OF CONTENTS

LIST OF FIGURES

LIST OF TABLES

LIST OF SCHEMES

CHAPTER I: INTRODUCTION

I.I Parkinson's Disease

Parkinson's Disease (PD) is the second most common neurodegenerative disease in the United States, after Alzheimer's, affecting more than 1% of people over the age of 60.[1] PD affects nearly 1 million people in the United States and more than 10 million worldwide, with most over the age of 65.[2,3] During diagnosis, physicians often describe PD as idiopathic, which means the cause is unknown.[3,4] Individuals affected by PD experience a decrease in dopamine production. Dopamine is a neurotransmitter that coordinates the body's movements, including the start and stop of voluntary and involuntary movements.[1] Without it, a PD patient will experience motor symptoms such as tremors, rigidity, bradykinesia (slow movement), and postural instability (balance problems), labeling the disease a "movement disorder."[5] Dopamine production originates from neurons in a region of the brain known as the substantia nigra.[6] The substantia nigra in the PD afflicted brain contains Lewy bodies, which are abnormal inclusions in the dying neuronal cells.[7] What are Lewy bodies though?

I.II Lewy Bodies

Lewy bodies are defined as an abnormal aggregation or clumping of a protein, which can be present in the brain in a range of neurologic diseases.[4] The location of these clumps makes a difference. There are no Lewy bodies within a healthy individual's

neuronal cell. However, in the neuronal cells of a PD patient, you will see a large Lewy body existing within the cytoplasm and causing the neuronal cell death.[8] Specifically for PD, these Lewy bodies are located in neuronal cells within the substantia nigra, and is what causes the four major motor symptoms of the disease.[4] People likely have Lewy bodies before the appearance of motor symptoms, and patients with more advanced PD symptoms often show more Lewy bodies. The two major components of Lewy bodies are phospholipids and the protein α-synuclein.[9] What is α-synuclein though, and what does it do?

I.III α-Synuclein

α-Synuclein is a 140-amino acid dense cytoplasmic presynaptic protein that plays a role in PD.[7] The primary structure of α-syn consists of three regions: 1) the N-terminus domain (amino acid residues 1-60), which contains a positively charged lysine residue, caries repeats of the highly conserved KTKEGV sequence; 2) the hydrophobic domain (residues 61-95), which is the central part of the protein, is known as the nonamyloid-beta component (NAC); 3) the C-terminus domain (residues 96-140), which is negatively charged and rich in acidic residues, is responsible for the disordered structure of the protein.[10-12] **Scheme 1** provides the sequence of α-synuclein. Although α-synuclein is a protein we all have in our bodies, the true role that it plays is still mostly unknown, but it is said that it must exist in advanced nerve cell functions.[13,14] There are several speculations about its functional role in the body, some of which include

neurotransmitter synthesis, calcium homeostasis, mitochondrial function, and gene regulation.[15] What is also unknown is how or why a normal α-synuclein protein becomes dysfunctional in PD patients. Scientists believe α-synuclein is mostly soluble in its natural form, but the protein in relation to this disease can become insoluble.[13] The reason for this insolubility is due to the NAC region (i.e. α-synuclein (61-95)) in the protein, studied by FT-IR and explained more in the following section.

MDVFMKGLSK AKEGVVAAAE KTKQGVAEAA GKTKEGVLYV GSKTKEGVVH GVATVAEKTK EQVTNVGGAV VTGVTAVAQK TVEGAGSIAA ATGFV*KKDQL GKNEEGAPQE GILEDMPVDP DNEAYEMPSE EGYQDYEPEA*

Scheme 1. The sequence of α-synuclein with the N-terminus underlined, the NAC region written regular, and the C-terminus in italics.

I.IV NAC (α-Synuclein (61-95))

α-Synuclein (61-95) is hydrophobic and known to be the source of aggregation within α-synuclein that causes Parkinson's Disease.[16] Previously in our group, α-synuclein (61-95) was synthesized, purified, and shown to be in an unstructured conformation in aqueous solution, sequence shown in **Scheme 2**.[17] α-Synuclein (61-95) was spread across an air-water interface, which has been widely used to mimic a cell membrane structure. Then, the α-synuclein (61-95) at air-water interface was studied by FT-IR spectroscopy, as shown in **Figure 1**.[17] The amide I band peak was observed at 1658 cm^{-1}, characteristic of an α-helical conformation for the secondary structure. Although

this result reveals that the membrane structure may provide the driving force for α-synuclein (61-95) to change from its unstructured conformation to an α-helix, the information from FT-IR is limited.[18] In addition, α-synuclein (61-95) displayed some challenges, as shown below.

E^{61}QVTNVGGAVVTGVTAVAQKTVEGAGSIAAATGFV^{95}

Scheme 2. The sequence of α-synuclein (61-95)

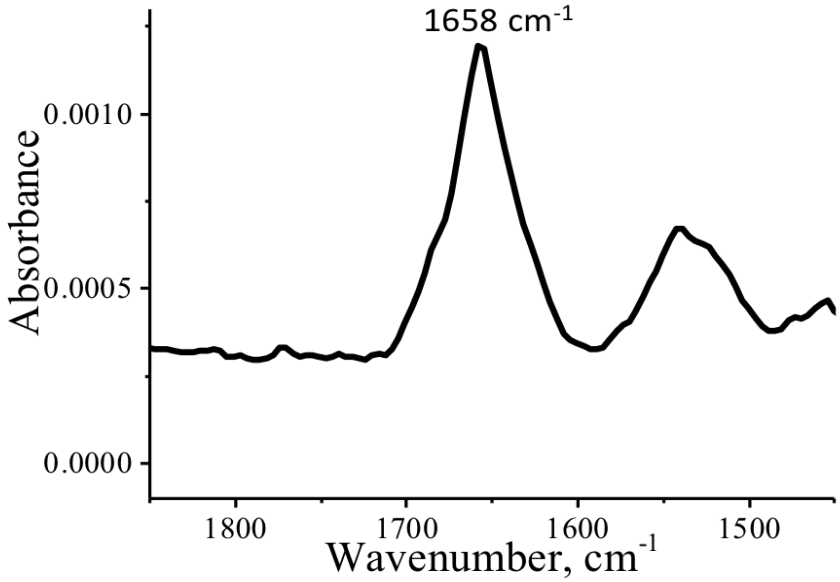

Figure 1. FT-IR results of Langmuir-Blodgett film of α-synuclein (61-95) transferred under 6 mN/m.[17]

I.V Problems of FT-IR to Determine Peptide Conformations

The three major conformations of peptides (also known as secondary structures) are: β-sheet, α-helix, and random coil/unstructured conformation.[19] The amide functional group of the polypeptide backbone absorbs infrared radiation, giving rise to

various characteristic amide bands in FT-IR spectroscopy.[17] Among these bands, the amide I band, stemming from the backbone carbonyl (C=O), is the most important band to address the conformation of peptides, as listed in **Table 1**.[20] It was observed that there were complications when trying to study α-synuclein (61-95) using FT-IR. These complications were that there was overlap between the band peaks of the secondary conformations in FT-IR.[21] In addition, a conformational change would cause a shift of various bands, such as the amide III band from the backbone C-N and the C-H bond on the α-carbon in the middle of the amino acid. Unfortunately, FT-IR cannot detect the shift in the amide III band and the C-H bond.[22] Where do these sensitive bands go? As we know, all vibrations are either infrared active or Raman active. The amide III band and other sensitive bands have been reported in Raman spectroscopy as described below.[20]

Table 1. Characteristic amide I frequencies of secondary structures of protein.[20]

Frequency (cm^{-1})	**Assignment**
1690-1680	β-sheet structure
1657-1648	α-helix
1645-1640	Unstructured
1630-1620	β-sheet structure

I.VI Raman Spectroscopy

Raman spectroscopy is also widely used to determine the conformation of proteins/peptides.[23] Raman spectroscopy measures relative frequencies at which a sample scatters radiation, unlike FT-IR spectroscopy which measures absolute

frequencies at which a sample absorbs radiation. In FT-IR, some wavelengths may be absorbed while others merely pass through the sample unaffected. Specific molecular bonds absorb a specific amount of energy and these losses of energy correspond to the peaks returned in an analysis. For Raman, the laser excites the bonds of a molecule, which generates measurable scattered light to identify the material in question.[24] In the Raman spectroscopy of proteins/peptides, there are four major amide bands: amide I band, amide II band, amide III band, and C_α–H_b band (summarized in **Table 2**).[25] Similar to FT-IR, the amide I band is comprised mainly of C=O stretching and is shown to be in the mid 1600's cm^{-1} range. The amide II band contains the N–H bending mode in Raman and is visible in the mid 1500's cm^{-1} range, however only for a random coil or β-sheet conformation. The amide III band in Raman spectroscopy is mainly composed of C–N stretching from the backbone amide bond. The position of the amide III band is only related to the conformation of local amide bonds without any coupling and is observed throughout the 1200's cm^{-1}.[26] The C_α–H_b band only contains the bending mode of the C_α–H bond and is observed in the 1400's cm^{-1} range.

Table 2. Band positions of various secondary structures in Raman spectroscopy in H_2O.[25]

Raman Bands	Random coil	α-helix	β-sheet
Amide I band position	1659-1682 cm^{-1}	1653-1658 cm^{-1}	1665-1675 cm^{-1}
Amide II band position	1548-1561 cm^{-1}	Not Available	1550-1564 cm^{-1}
Amide III band position	1241-1250 cm^{-1}	1268-1298 cm^{-1}	1220-1248 cm^{-1}
C_α–H_b band position	1445-1482 cm^{-1}	1445-1482 cm^{-1}	1445-1482 cm^{-1}

I.VII Problems with α-Synuclein (61-95)

During our research, we found that the major problem in the spectroscopic study of α-synuclein (61-95) is the low solubility, at only 0.2 mg/mL. In addition, although Raman spectroscopy is capable of determining more amide bands of the conformational change of peptides than FT-IR, the signal is usually low due to the peptide's low solubility.[27] Therefore, a good solubility, starting in the 10mg/mL range, is required to shift our research from FT-IR to Raman spectroscopy for α-synuclein (61-95). Furthermore, various segment peptides of α-synuclein have been detected in Lewy bodies. Hence, there is a need to synthesize segments of the NAC at different lengths and study their biophysical behavior to help determine how to increase the solubility. This will help increase the Raman signal to allow a more confident study of the amide bands to study the structure of α-synuclein. These peptides will be synthesized in the lab via peptide synthesis using fmoc-preprotected amino acids. In general, the goal is to increase the solubility of the NAC region.

I.VIII Thesis Proposal

The goal of my thesis was to study the solubility of various segments of the protein α-synuclein's (61-95), the NAC region, and observe if any had greater solubility as well as to evaluate the Raman spectroscopy results of samples dissolved in water. As mentioned in Section 1.3, α-synuclein (61-95) contains hydrophobic amino acid residues, whereas the N- and C-termini contain more hydrophilic residues.[10-12] Therefore, both shorter and

longer length peptides of α-synuclein will be synthesized. Shorter peptides contain less hydrophobic residues, and thus solubility may be improved. Longer peptides contain more hydrophilic residues, which could also improve the solubility. It is reported that residues 71-82 of α-synuclein (61-95) is the critical sequence for the dysfunction of α-synuclein.[28] However, residues 57-102 has also attracted wide scientific attention. Therefore, the peptides studied in this thesis include: α-synuclein (71-82), α-synuclein (57-102), and α-synuclein (66-85), which is the average of α-synuclein (61-95) and α-synuclein (71-82). The sequences of the three peptides are shown below in **Schemes 3-5**. The peptides were synthesized, purified, and studied by Raman spectroscopy as the details are described in **Chapter II**.

$$V^{71}TGVTAVAQKTV^{82}$$

Scheme 3. The sequence of α-synuclein (71-82)

$$V^{66}GGAVVTGVTAVAQKTVEGA^{85}$$

Scheme 4. The sequence of α-synuclein (66-85)

$$E^{57}KTKEQVTNVGGAVVTGVTAVAKTVEGAGSIAAATGFVKKDQLGK^{102}$$

Scheme 5. The sequence of α-synuclein (57-102)

CHAPTER II: MATERIALS AND METHODS

II.I Materials

The materials, their purity, and their respective suppliers are as follows. Fmoc-L-Alanine (99.91%), N^{α}-Fmoc-N^{γ}-trityl-L-Asparagine (99.69%), N^{α}-Fmoc-N^{δ}-trityl-L-Glutamine (99.61%), Fmoc-L-Glutamic acid γ-*tert*-butyl ester hydrate (99.11%), Fmoc-Glycine (99.37%), Fmoc-L-Leucine (99.80%), N^{α}-Fmoc-N^{ε}-Boc-L-Lysine (99.84%), Fmoc-*O*-*tert*-butyl-L-Serine (99.83%), Fmoc-L-Valine (99.53%), and Rink amide MBHA Resin (0.3-0.8 meq/g, 200-400 mesh) (>99.00%) all came from Chem-Impex International based in Wood Dale, IL.[29-38] N^{α}-Fmoc-L-Aspartic acid α-*tert*-butyl ester (99.69%) and N^{α}-Fmoc-L-Isoleucine (>98.00%) both were purchased from Novabiochem (Hohenbrunn, Germany).[39,40] Fmoc-Phe-OH (>99.00%) came from BACHEM in Torrance, CA.[41] Both Fmoc-Thr(tBu)-OH (99.60%) and 1-hydroxybenzotriazole hydrate (HOBt hydrate) (>99.00%) came from Anaspec Inc. (Fremont, CA).[42,43] Dichloromethane (DCM) (99.60%), Acetonitrile-HPLC grade (99.95%), N,N-dimethylformamide (DMF) (99.80%), Ethyl Ether Anhydrous (Diethyl ether) (99.90%), and Acetic Anhydride (99.80%) were purchased from Fisher Scientific, (Fairlawn, NJ).[44-48] Piperidine (99.00%) and Triisopropysilane (98.00%) came from Sigma-Aldrich based in St. Louis, MO.[49,50] N,N'-Diisopropylcarbodiimide(DIC) (99.00%) and Trifluoroacetic acid(TFA) (99.00%) came from Alfa Aesar (Ward Hill, MA).[51,52] The ultra-high purity Nitrogen gas (99.99%) came from NexAir (Memphis, TN).[53]

II.II Peptide Synthesis

Solid phase peptide synthesis was used to synthesize the peptides observed in this thesis. A CEM discover bio manual microwave peptide synthesizer (**Figure 2**) was used in conjunction with Rink Amide MBHA resin as the solid support. The protection strategy used during synthesis is known as fluorenylmethyloxycarbonyl (Fmoc) chemistry. Each amino acid came preprotected at its amino terminus with an Fmoc group, which was used to protect the amine group of the amino acids by preventing solution coupling of dissolved amino acids. Fmoc is mild, flexible, and versatile, offering much more synthetic option than say tert-butyloxycarbonyl (Boc) chemistry.

The desired peptide was synthesized from C-terminus to N-terminus by repeating the sequence coupling-washing-deprotection-washing-cleavage as shown in **Figures 3-5**. During the coupling stage, the peptide was assembled starting with the carboxylic acid terminus of the Fmoc-amino acid being activated and coupled to the growing chain. The coupling of the first amino acid involves the coupling of the C-terminal of the amino acid of the active sites on the surface of 2 molar equivalents of the Rink Amide resin. Hydroxybenzotriazole (HOBt) was then added to suppress racemization, followed by the addition of Diisopropylcarbodiimide (DIC) to activate the carboxylate. The amine group on the surface of the solid phase then reacted with the activated carboxylate to form an amide bond. N,N-dimethylformamide (DMF) was then used multiple times to wash the resin and to clean the surface of the solid phase.

During the deprotection stage, Fmoc deprotection was initiated by utilizing a treatment of 20% piperidine in (DMF) (v/v). Piperidine reacted and attached to the Fmoc

group protecting the amine. As a result, the amine group was now deprotected and ready to be coupled to the next amino acid. DMF was then again used multiple times to wash the resin and to clean the surface of the solid phase.

The coupling and deprotection process was repeated until all amino acids were added to the desired peptide. Once the desired peptide chain was complete, the peptide was capped by being treated with acetic anhydride and DCM. The peptide was then removed from the Rink Amide MBHA resin by suspending it into a 20 mL solution, in the volume ratios of 75: 22: 1.5: 1.5 volumes of TFA, DCM, triisopropylsilane and H_2O, respectively. During this process, side chain protecting groups were removed, such as Boc and tBu, yielding on the linear crude peptide. The H_2O and triisopropylsilane were utilized to prevent side reactions with reactive cationic species released as a result of the side chain deprotections.

Nitrogen purging was used to remove the wash solution of TFA, DCM, triisopropylsilane and H_2O. Diethyl ether was subsequently added to the peptides prior to a centrifugation step. The liquid in the centrifuge tube was decanted, and the precipitate was the final product of the desired crude synthetic peptide.

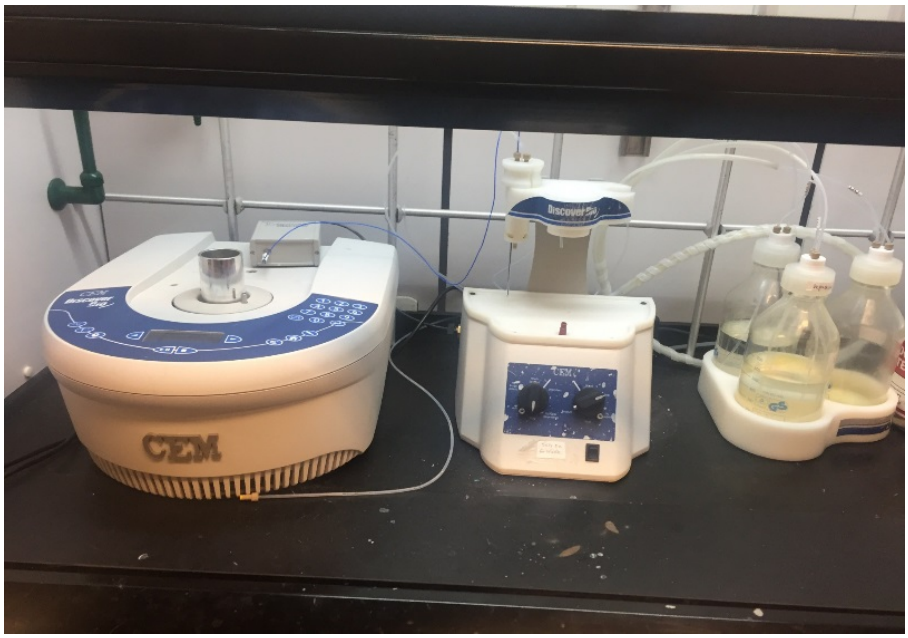

Figure 2. CEM Discover bio manual microwave peptide synthesizer

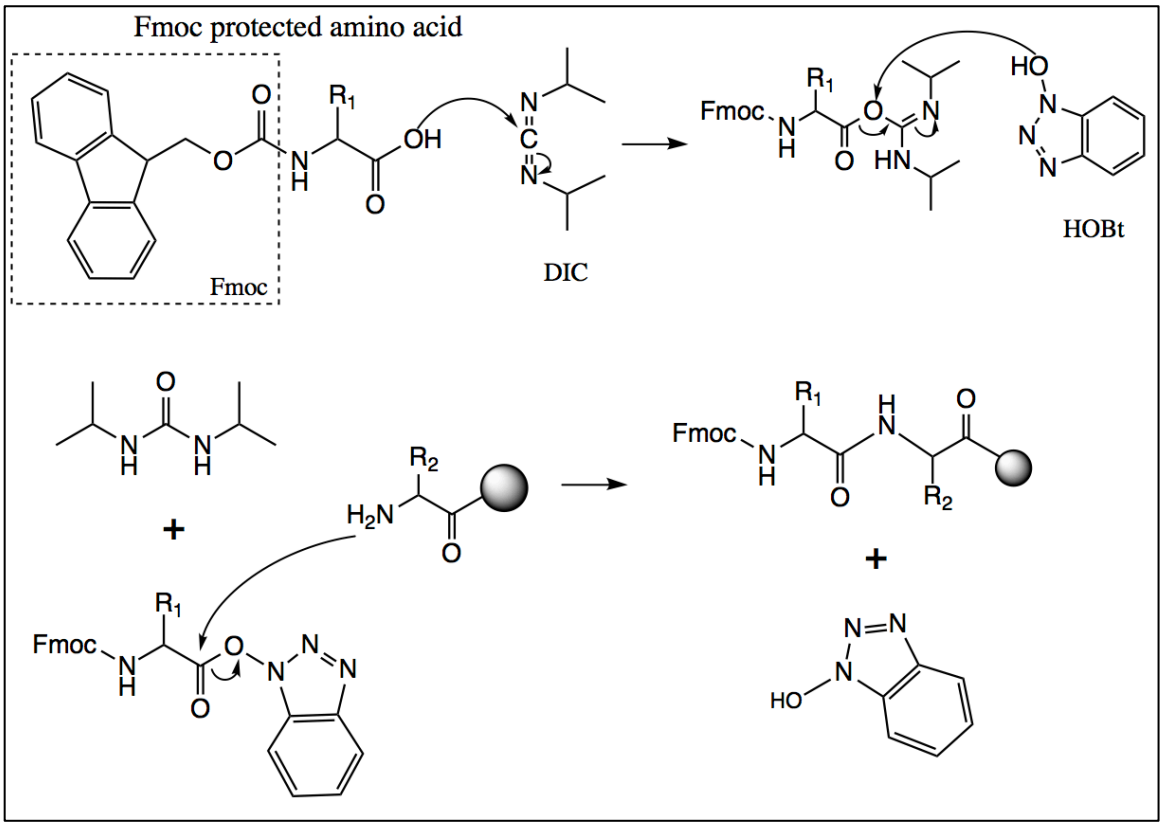

Figure 3. Coupling reaction during peptide synthesis

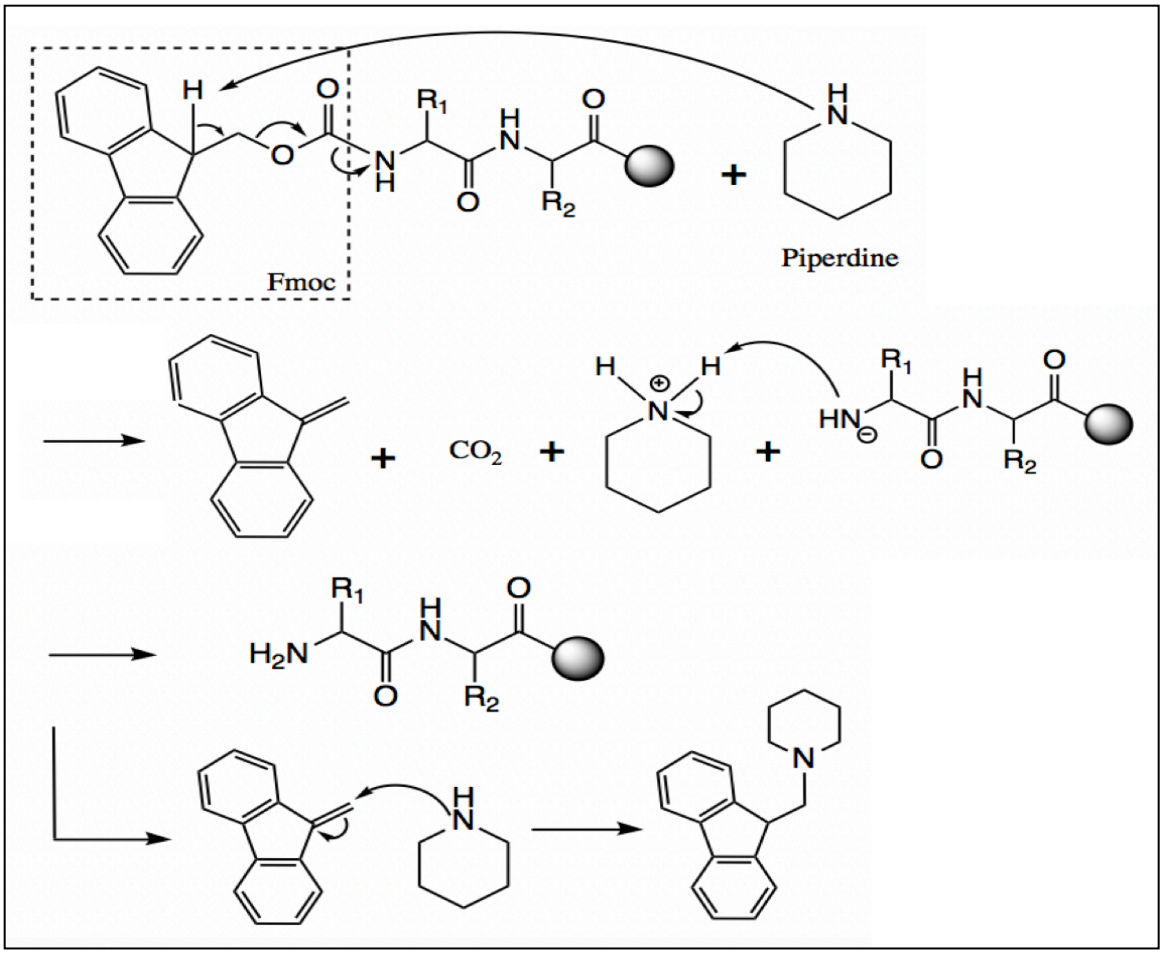

Figure 4. Deprotection reaction during peptide synthesis

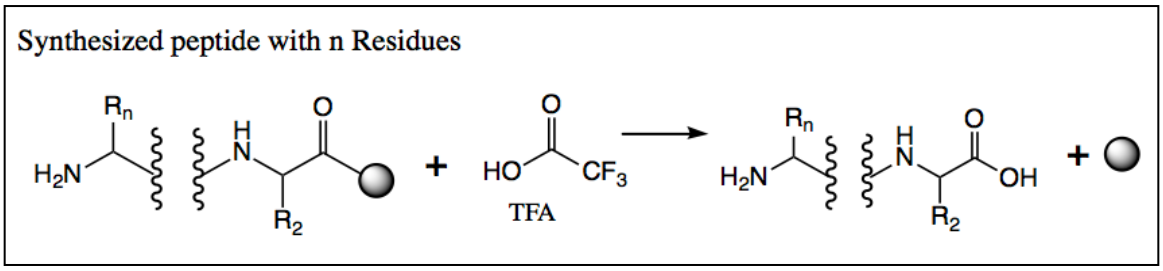

Figure 5. Cleavage reaction during peptide synthesis

II.III High Pressure Liquid Chromatography (HPLC)

The HPLC purification in this thesis was performed using two different instruments. A-Synuclein (71-82) and α-synuclein (66-85) were both purified using a Waters 1525 Binary Solvent Pump attached to a Phenomenex Reverse Phase Semi Prep C18 Column, Jupiter Model 00G-4055- P0 with the column's internal diameter at 21.5 mm and with a length of 250 mm. The Pump was attached to a Waters 2489 UV-Vis detector and detected the UV absorption using a wavelength of 210nm. The Waters 1525 Binary Solvent Pump and the Waters 2489 UV-Vis detector are shown in **Figure 6**. Mobile phase A was a solution of 18.2 Ω deionized water to 0.1% TFA (v/v) and the mobile phase B was a solution of HPLC grade acetonitrile to 0.1% TFA (v/v). α-Synuclein (57-102) was purified using a Varian Prepstar SD-1 pump with a Supelco Ascentis C18 column (5 μM; 25 cm x 21.2 mm; Sigma-Aldrich 581347-U), shown in **Figure 7**. A solution of 18.2 Ω deionized water to 0.05% TFA (v/v) was used for mobile phase A and a solution of HPLC grade acetonitrile to 0.05% TFA (v/v) was used for mobile phase B.

Method development was performed for each peptide in order to separate the pure peptide precisely. **Figure 8** shows the method for separation of each peptide from the impurities in the crude product. The purification of α-synuclein (71-82) was achieved by a ratio of a linear gradient of 25-80% by volume of A and B at a flow rate of 21.2 mL/minute for 8 minutes. A-Synuclein (66-85) was purified using a linear gradient ratio of 34-39% by volume of A and B for 8 minutes with a flow rate of 21.2 mL/minute. Lastly, the purification of α-synuclein (57-102) was achieved by a linear gradient ratio of 30-100%

by volume of A and B at a flow rate of 10.0 mL/minute for 10 minutes. Once each purified peptide was collected, they were frozen at -80 ° C and then lyophilized to obtain the solid form of the purified peptides.

Figure 6. Waters 1525 Binary HPLC pump with Waters 2489 UV/Visible detector

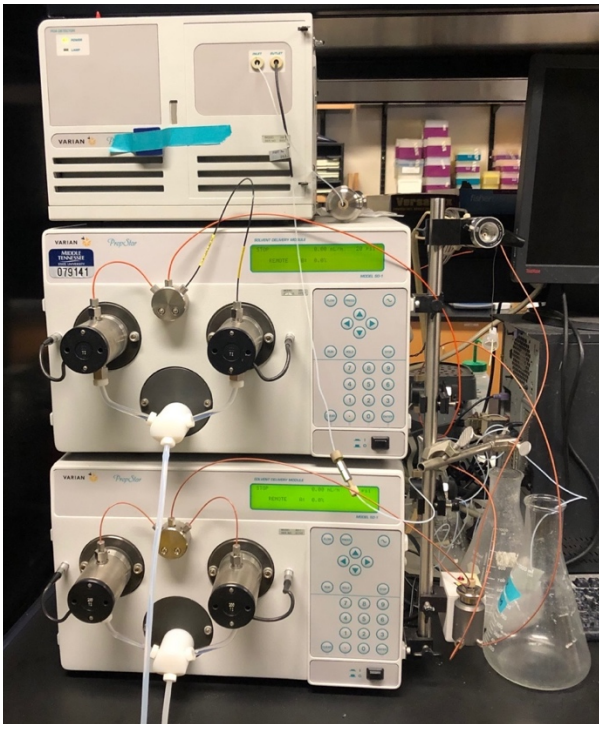

Figure 7. Varian Prepstar SD-1 with Supelco Ascentis C18 column

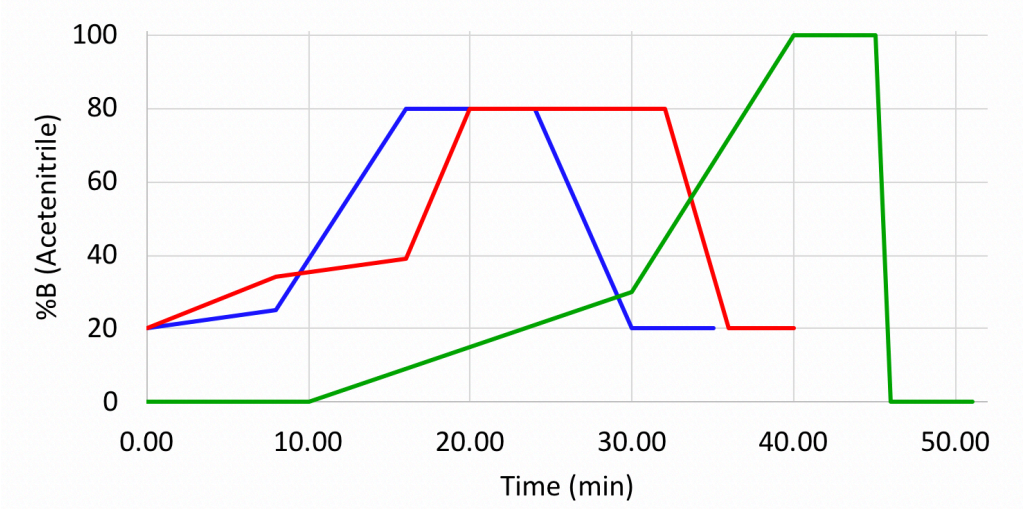

Figure 8. Comparison of HPLC method sets for α-synuclein (71-82) (blue), α-synuclein (66-85) (red), and α-synuclein (57-102) (green)

II.IV Mass Spectrometry

Mass spectrometry (MS) is a powerful technique that can identify a wide variety of chemical compounds. It is used determine the molecular mass and the elemental composition of a sample, and the chemical structures of larger molecules. The success of the synthesis and purification of each peptide was confirmed by MS from a Waters SYNAPT q-TOF tandem mass spectrometer, as shown in **Figure 9**. This instrument was used for all the mass spectrometric measurements carried out in this thesis. Each peptide was added in water and sonicated until dissolved before analyzing the mass. A 100 μL syringe was used to collect the sample. The sample cone temperature for the MS was at 150 °C and the capillary voltage was set to 3 keV. N_2 was used at a rate of 500 L/hour to evaporate the aqueous peptide solution containing 0.1% of TFA. The flow rate was set to 20 μL/minute. The run duration and scan time were set to 0.5 minutes and 0.5 seconds, respectively. The positive ion mode was used for the MS measurements.

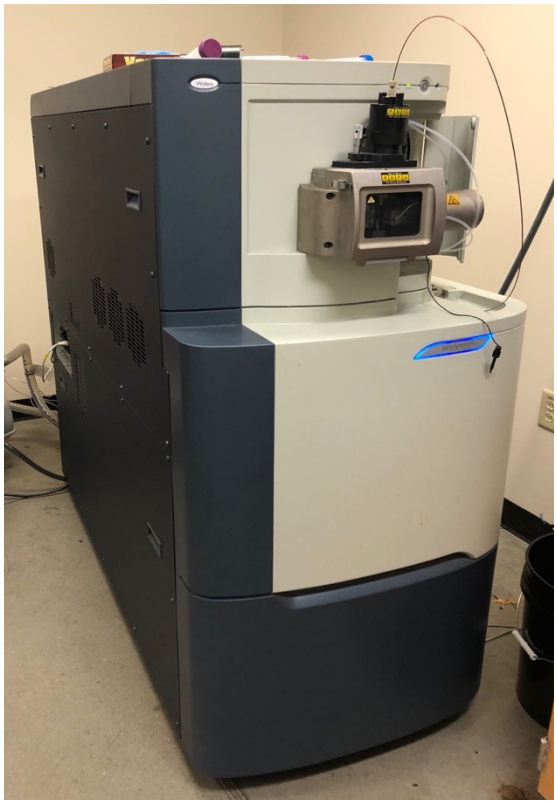

Figure 9. Waters Synapt tandem mass spectrometer with time-of-flight configuration

II.V Raman Spectroscopy

Raman Spectroscopy was performed in this thesis using a LabRAM HR Evolution confocal Raman microscope, **Figure 10**. This instrument is equipped with a 785 nm excitation laser and a 532 nm excitation laser, but only the 532 nm excitation laser was used in this thesis. Once the instrument is turned on and the lasers are warmed up, an auto-calibration must be performed using a silicon wafer. This auto-calibration was performed using the 532 nm laser at 0.01% laser power (ND filter) and a grating of 600 grooves/mm. For each peptide, the Raman spectra of the solid peptide was obtained

first, followed by the peptide in aqueous solution. The objective of the microscope was used at x50_VIS_LWD throughout all data collected.

For the solid form of α-synuclein (71-82), the Raman spectra was collected using an acquisition time of 5 seconds, accumulations set at 10, the ND filter set at 25%, and the grating set at 600 grooves/mm. For the aqueous solution of α-synuclein (71-82), the best results were obtained using an acquisition time of 10 seconds, accumulations set at 20, the ND filter set at 1%, and the grating set at 600 grooves/mm. The Raman spectra of the solid form of α-synuclein (66-85) was obtained using an acquisition time of 5, accumulation set of 10, the ND filter set at 100%, and the grating set at 1800 grooves/mm. α-Synuclein (66-85) in aqueous solution achieved the best results using an acquisition time of 5 seconds, accumulations set at 10, the ND filter set at 50%, and the grating set at 1800 grooves/mm. The Raman Spectra of α-synuclein (57-102) in solid form was obtained using an acquisition time of 3, accumulations set at 10, the ND filter set at 100%, and the grating set at 1800 grooves/mm. Lastly, the aqueous solution of α-synuclein (57-102) achieved its best Raman spectra using an acquisition time of 5, accumulations set at 10, the ND filter set at 100%, and the grating set at 600 grooves/mm.

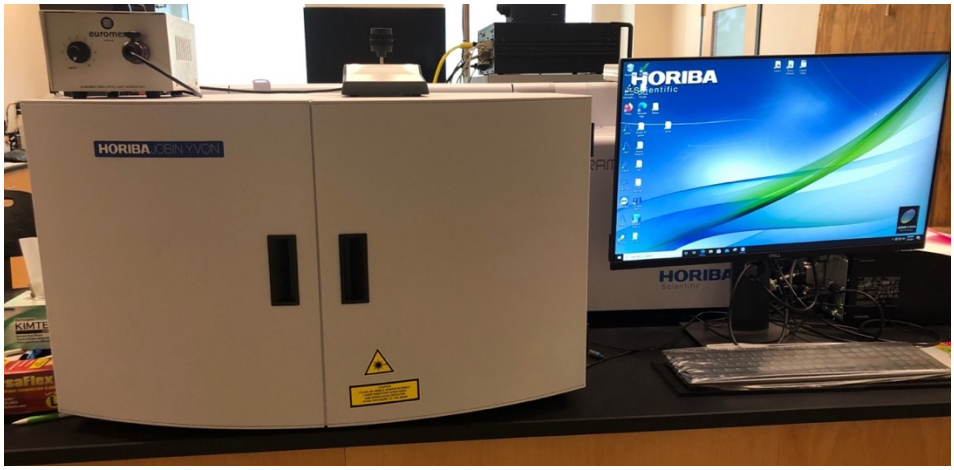

Figure 10. LabRAM HR Evolution confocal Raman microscope with 532 nm excitation laser

CHAPTER III: RESULTS & DISCUSSION

III.I Solubility

Before each peptide could be purified via HPLC, it had to be dissolved in DI water. Each sample was dissolved to try to determine the maximum solubility of each. Once the maximum solubility was reached, 20% of acetonitrile was added to assist in the purification process. **Table 3** shows the following data. To prepare 10 mg of α-synuclein (71-82) for HPLC purification, it took 6.75 mL of DI water and 1.5 mL of acetonitrile. To prepare 10 mg of α-synuclein (66-85) for HPLC purification, it took 13.5 mL of DI water and 3mL of acetonitrile. To prepare this peptide for HPLC purification, it only needing 1.6 mL of DI water and 0.3 mL of acetonitrile.

A-Synuclein (71-82) had a solubility of 1.48 mg/mL when dissolved in DI water. A-Synuclein (66-85) was the least soluble of the three peptides, but still more soluble than that of the NAC region. The observed solubility of this peptide in DI water was lower than α-synuclein (71-82) at only 0.74 mg/mL. Lastly, α-synuclein (57-102) was the most soluble of the three peptides that were studied. α-Synuclein (57-102) had an observed solubility of 6.25 mg/mL when dissolved in DI water. **Figure 11** helps provide a visual for the solubility each sample as compared to the solubility of the NAC (α-Synuclein (61-95)), which again only had a solubility of 0.2 mg/mL.

Table 3. HPLC preparation for 10mg of sample once maximum solubility was reached

	α-synuclein (71-82)	α-synuclein (66-85)	α-synuclein (57-102)
DI H2O (mL)	6.75	13.5	1.6
ACN (mL)	1.5	3	0.3

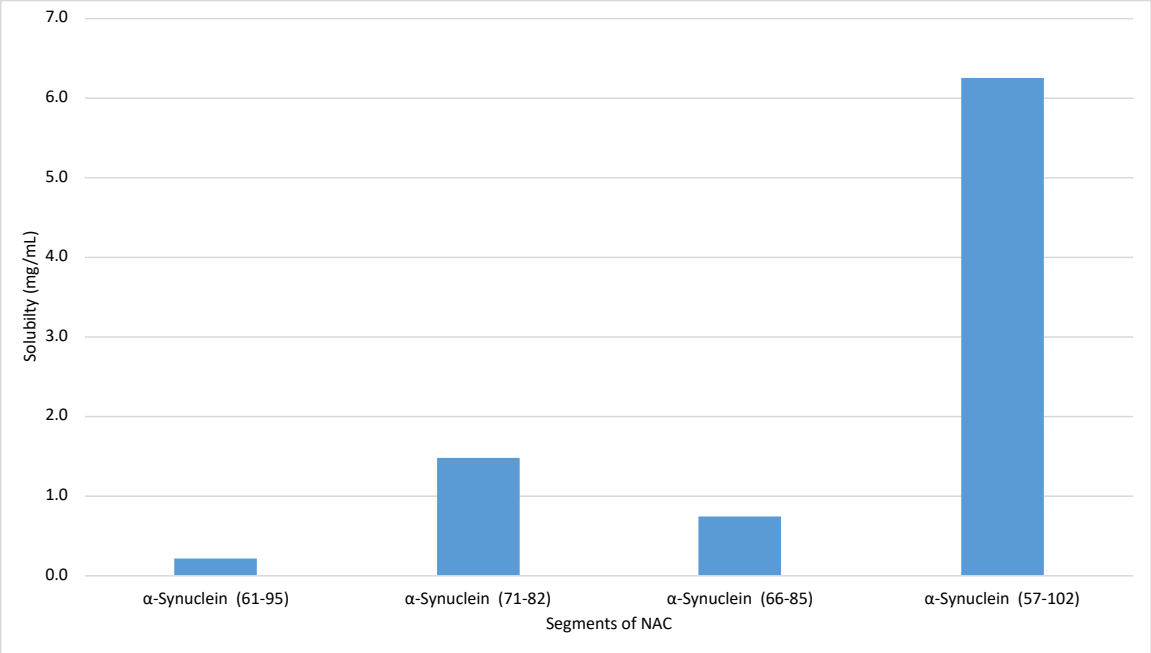

Figure 11. Comparison of solubility of different length NAC segments when dissolved in DI water

III.II α-Synuclein (71-82)

The HPLC chromatogram of the α-synuclein (71-82) is shown in **Figure 12**. The purified form of the peptide had a maximum absorbance of approximately 1.60 AU. It also had a retention time of 7.8-8.8 minutes, which means it only took about 24.5-25.5% acetonitrile to elute. When the α-synuclein (71-82) was synthesized, it had a theoretical mass of 1215.33 Da. **Figure 13** shows the mass spectrum of purified α-synuclein (71-82)

in its singularly charged form, with an actual mass of 1214.87 Da. Since the mass spectrum was so pure, it is reasonable to suggest that the synthesis was successful, and the purification method was effective.

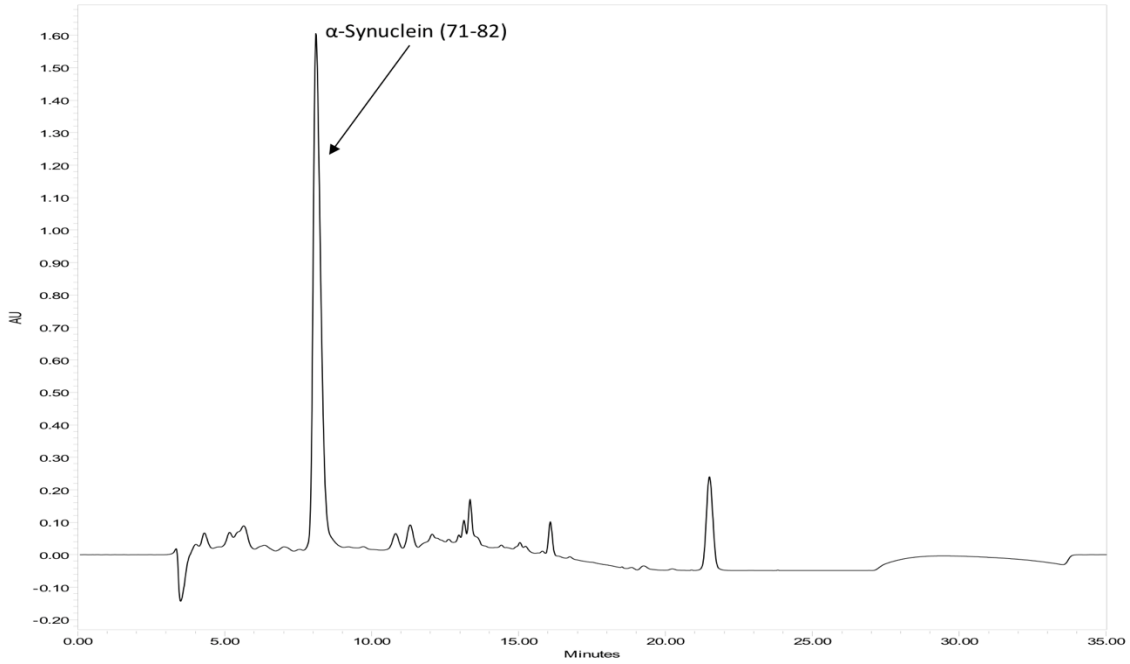

Figure 12. HPLC chromatogram of purifying α-synuclein (71-82)

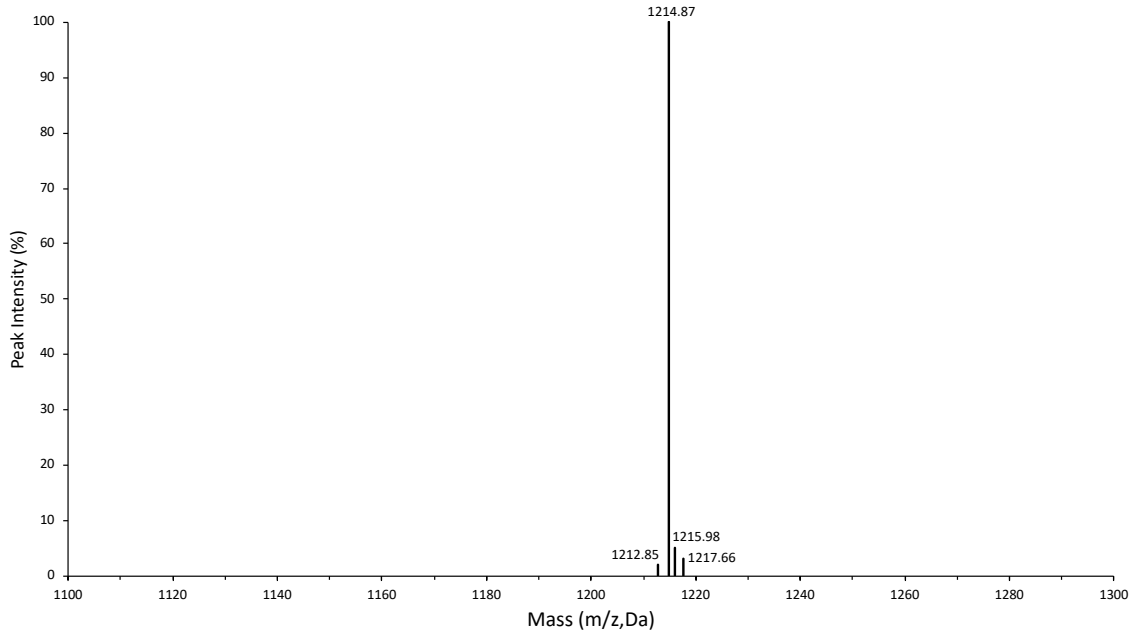

Figure 13. Mass spectrum of purified α-synuclein (71-82)

The Raman spectrum of the purified α-synuclein (71-82) in solid form is shown in **Figure 14**. The amide I band peak was observed at ~1667 cm^{-1}, the amide II band peak was observed at ~1555 cm^{-1}, the amide III band peak was observed at ~1232 cm^{-1}, and the C_α–H_b band peak was observed at ~1450 cm^{-1}. **Figure 15** displays the Raman spectrum of the purified α-synuclein (71-82) dissolved in water. In this spectrum however, the band peaks were much weaker due to a lack of solubility. The amide I band peak was observed at ~1659 cm^{-1}, the amide II band peak was observed at ~1556 cm^{-1}, the amide III band peak was not able to be identified, and the C_α–H_b band peak was observed at ~1453 cm^{-1}.

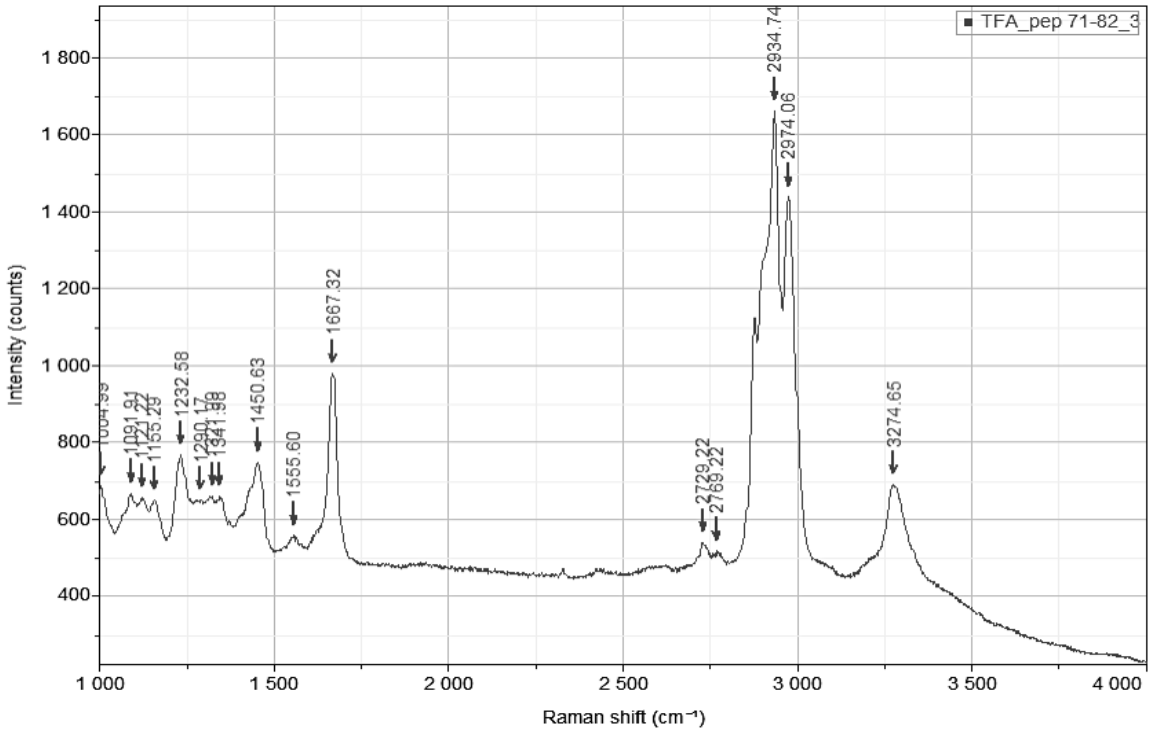

Figure 14. Raman Spectrum of purified α-synuclein (71-82) in solid form

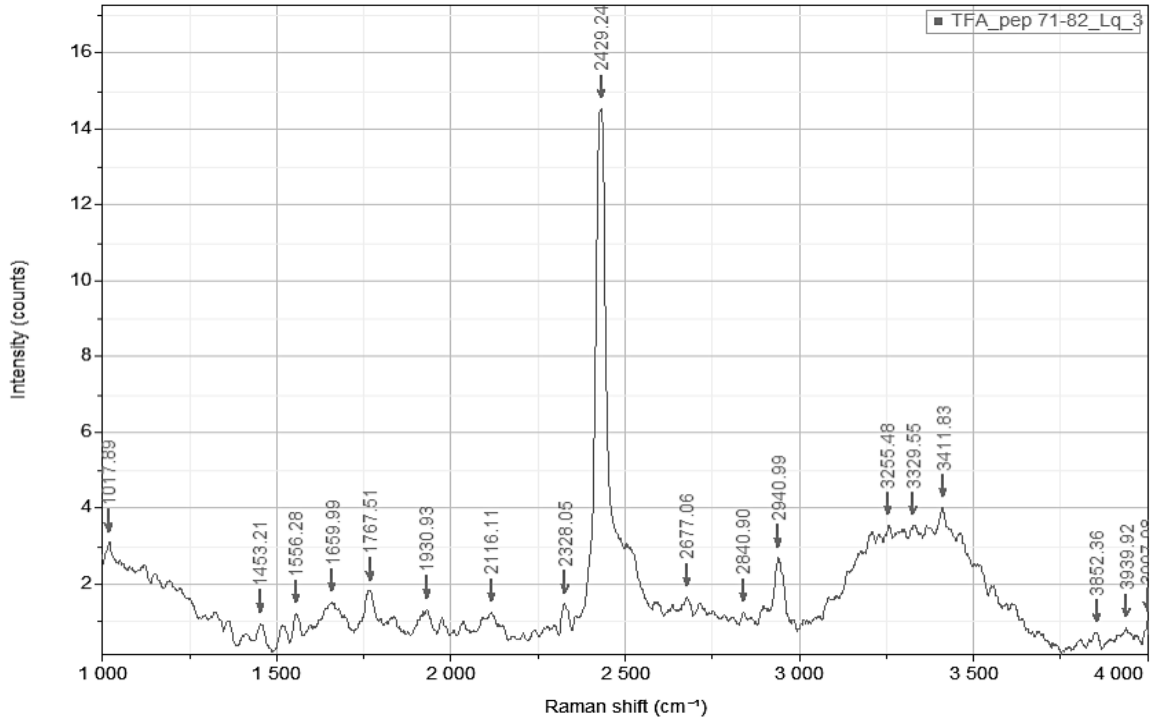

Figure 15. Raman spectrum of purified α-synuclein (71-82) dissolved in DI water

III.III α-Synuclein (66-85)

The HPLC chromatogram of the α-synuclein (66-85) is shown in **Figure 16**. The purified form of the peptide had a maximum absorbance of only about 0.105 AU. It had 2 retention times, one at 10.3-11.6 minutes and the second one at 12.0-13.0 minutes, possibly due to isomerization. This means it took between 35.4-37.1% acetonitrile to elute α-synuclein (66-85). When the α-synuclein (66-85) was synthesized, it had a theoretical mass of 1855.99 Da. **Figure 17** shows the mass spectrum of α-synuclein (66-85) in its singularly and doubly charged forms. Its singularly charged ion had an actual mass of 1856.03 Da, and its doubly charged form had a mass of 929.49 Da. It can be concluded that the synthesis was successful, and the purification was good, since the mass spectrum was without any impurity peaks.

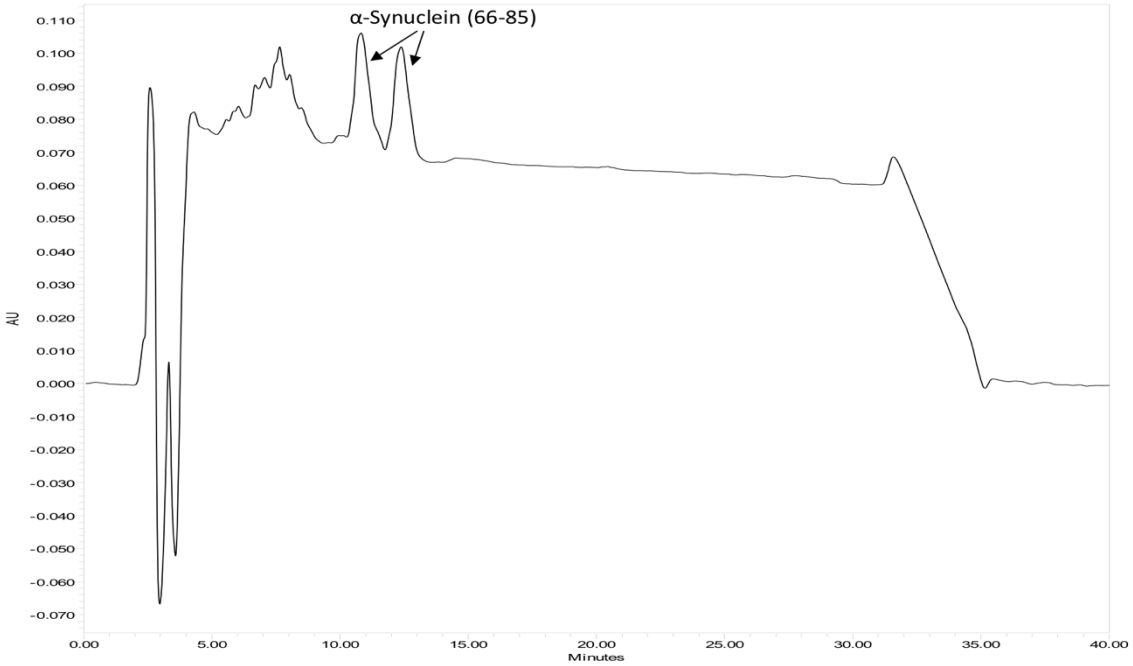

Figure 16. HPLC chromatogram of purifying α-synuclein (66-85)

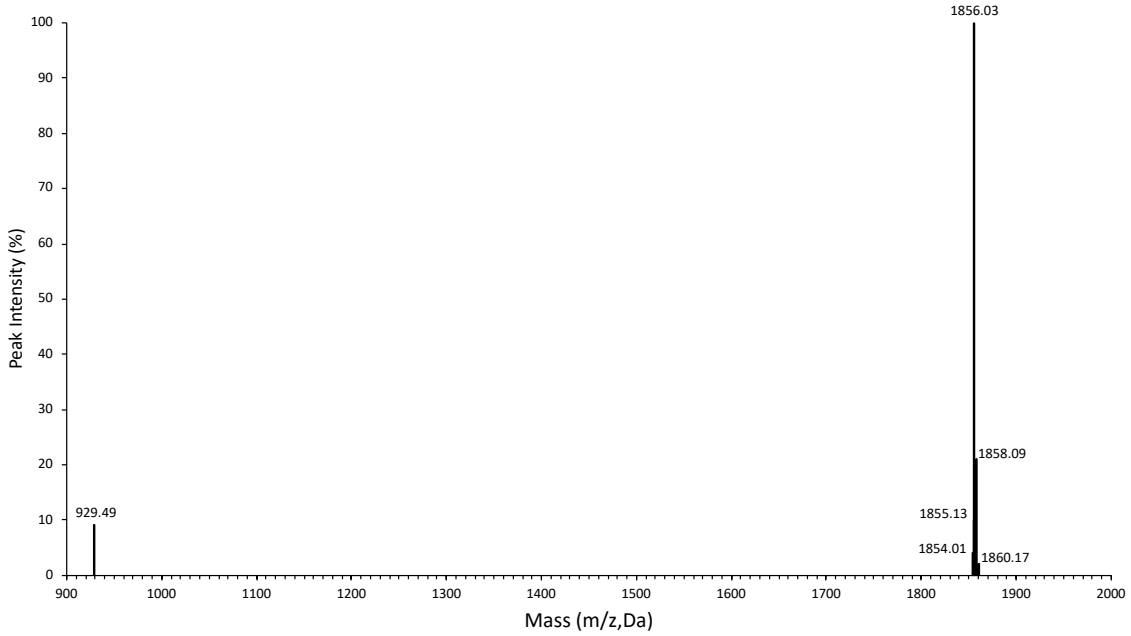

Figure 17. Mass spectrum of purified α-synuclein (66-85)

The Raman spectrum of the purified α-synuclein (66-85) in solid form is shown in **Figure 18**. The amide I band peak was observed at ~1669 cm^{-1}, the amide II band peak was observed at ~1555 cm^{-1}, the amide III band peak was observed at ~1233 cm^{-1}, and the C_α–H_b band peak was observed at ~1449 cm^{-1}. The Raman spectrum of the purified α-synuclein (66-85) dissolved in water is shown in **Figure 19**. Similar to α-synuclein (71-82), the band peaks were much weaker than that of the solid form due to a lack of solubility. The amide I band peak was observed at ~1667 cm^{-1}, the amide II band peak was observed at ~1554 cm^{-1}, the amide III band peak was observed at ~1215 cm^{-1}, and the C_α–H_b band peak was observed at ~1448 cm^{-1}.

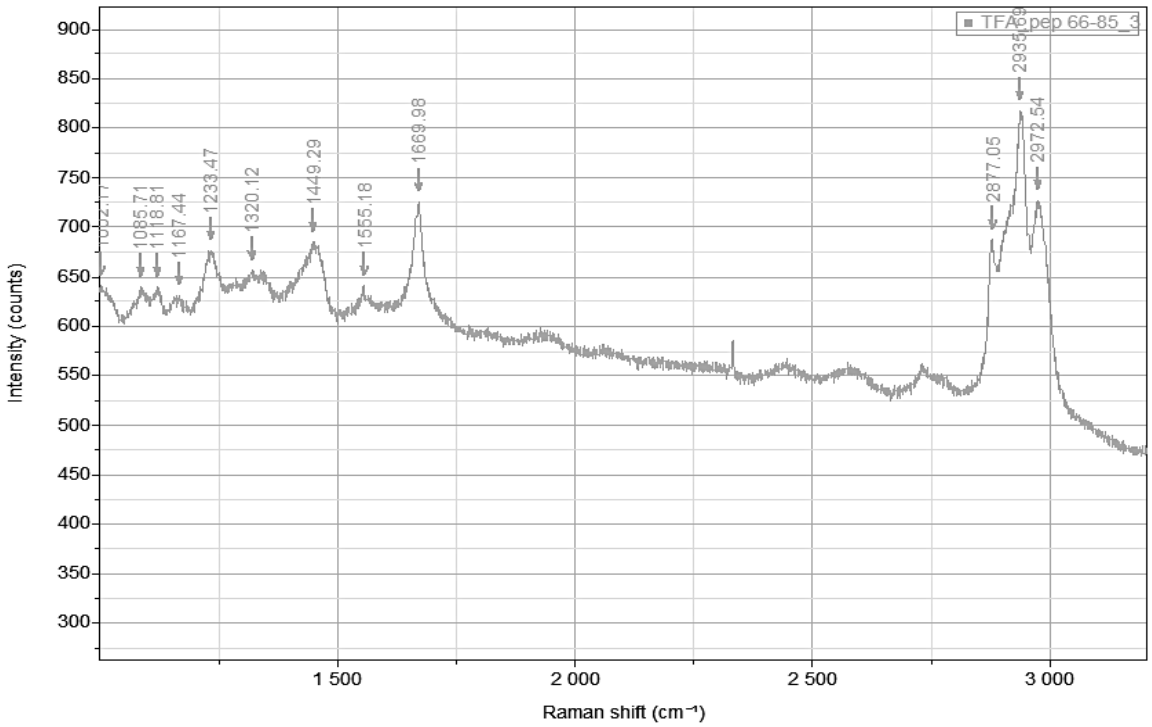

Figure 18. Raman Spectrum of purified α-synuclein (66-85) in solid form

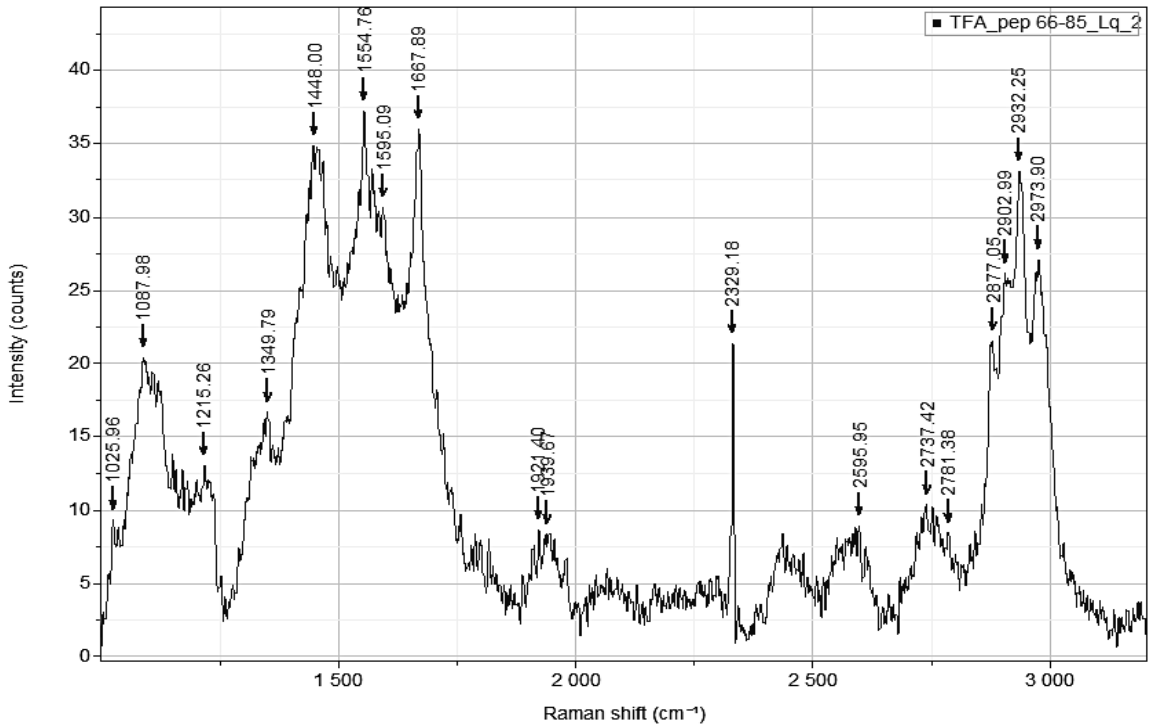

Figure 19. Raman Spectrum of purified α-synuclein (66-85) dissolved in DI water

III.IV α-Synuclein (57-102)

The HPLC chromatogram of the α-synuclein (57-102) is shown in **Figure 20**. The purified form of the peptide had a maximum absorbance of approximately 0.52 AU. It also had a retention time of 37.7-39.8 minutes, which means it took about 83.9-98.6% acetonitrile to elute. When the α-synuclein (57-102) was synthesized, it had a theoretical mass of 4586.98 Da. **Figure 21** shows the mass spectrum of α-synuclein (57-102) in its singularly and triply charged forms. Its singularly charged ion had an actual mass of 4585.51 Da and its triply charged form had a mass of 1531.94 Da. Similar to the other two peptides synthesized, since the mass spectrum was free of impurity peaks, it is inferred that both the synthesis and the purification were effective.

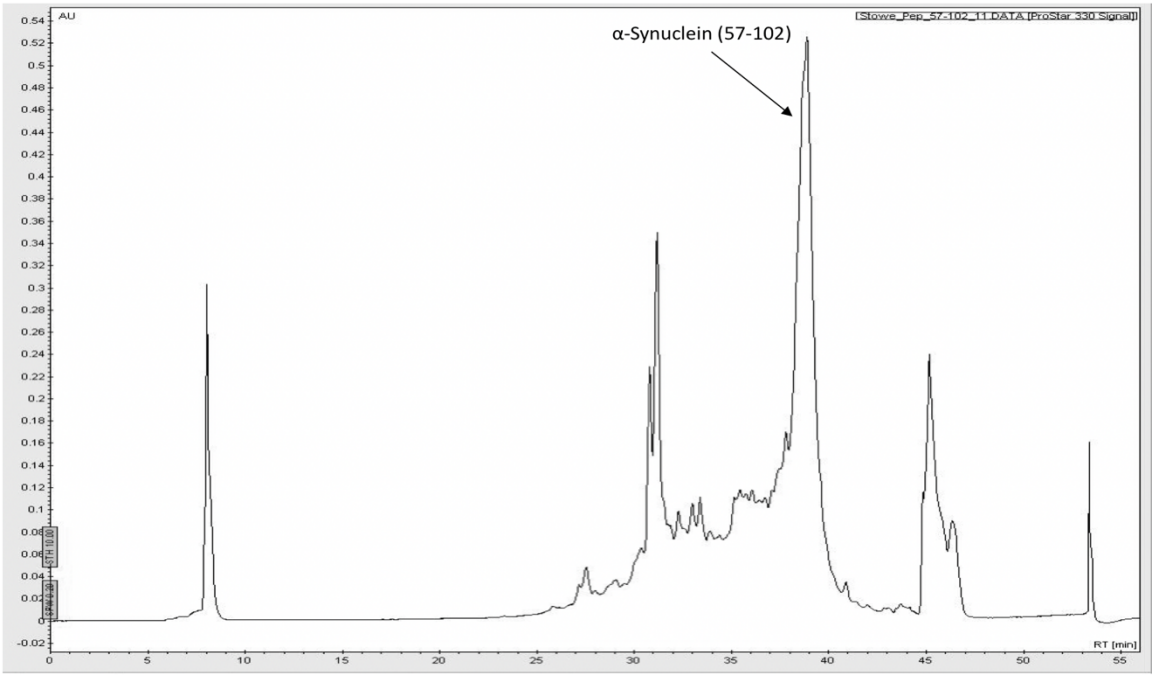

Figure 20. HPLC chromatogram of purifying α-synuclein (57-102)

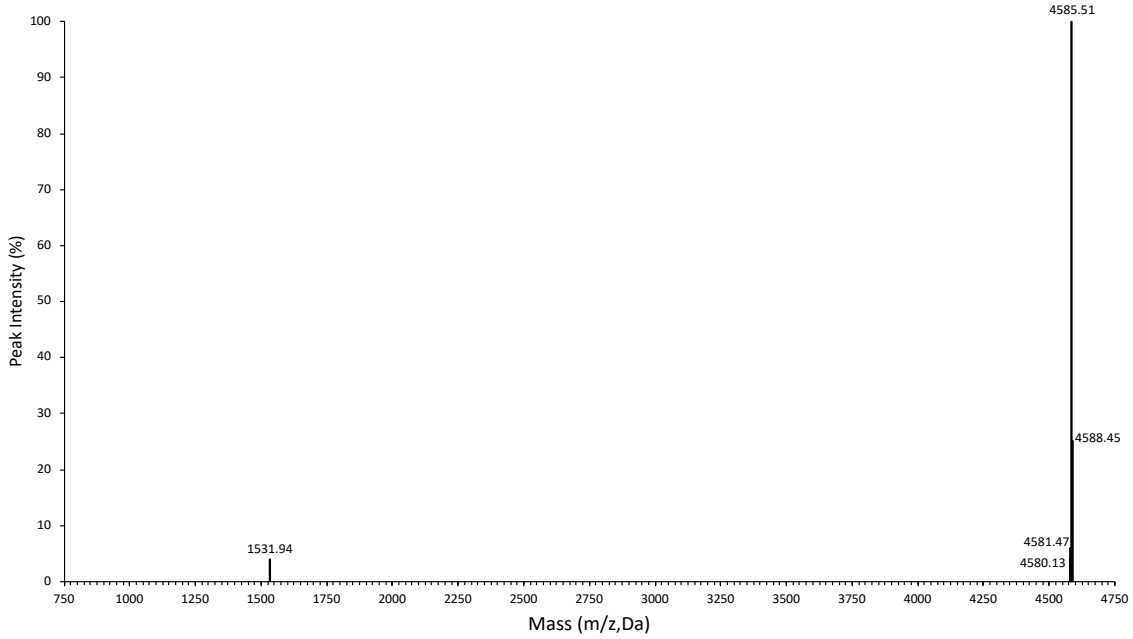

Figure 21. Mass spectrum of purified α-synuclein (57-102)

The Raman spectrum of the purified α-synuclein (57-102) in solid form is shown in **Figure 22**. The amide I band peak was observed at ~1673 cm^{-1}, the amide II band peak was observed at ~1570 cm^{-1}, the amide III band peak was observed at ~1228 cm^{-1}, and the C_α–H_b band peak was observed at ~1438 cm^{-1}. **Figure 23** displays the Raman spectrum of the purified α-synuclein (57-102) dissolved in water. Here, since the solubility for α-synuclein (57-102) was 4x larger than that of α-synuclein (71-82) and 8x larger than α-synuclein (66-85)'s (as seen in **Figure 11)**, the band peaks were much more defined. The amide I band peak was observed the same as in the solid state at ~1670 cm^{-1}, the amide II band peak was observed at ~1608 cm^{-1}, the amide III band peak was observed the same as the solid state at ~1227 cm^{-1}, and the C_α–H_b band peak was observed the same as the solid state as well at ~1447 cm^{-1}.

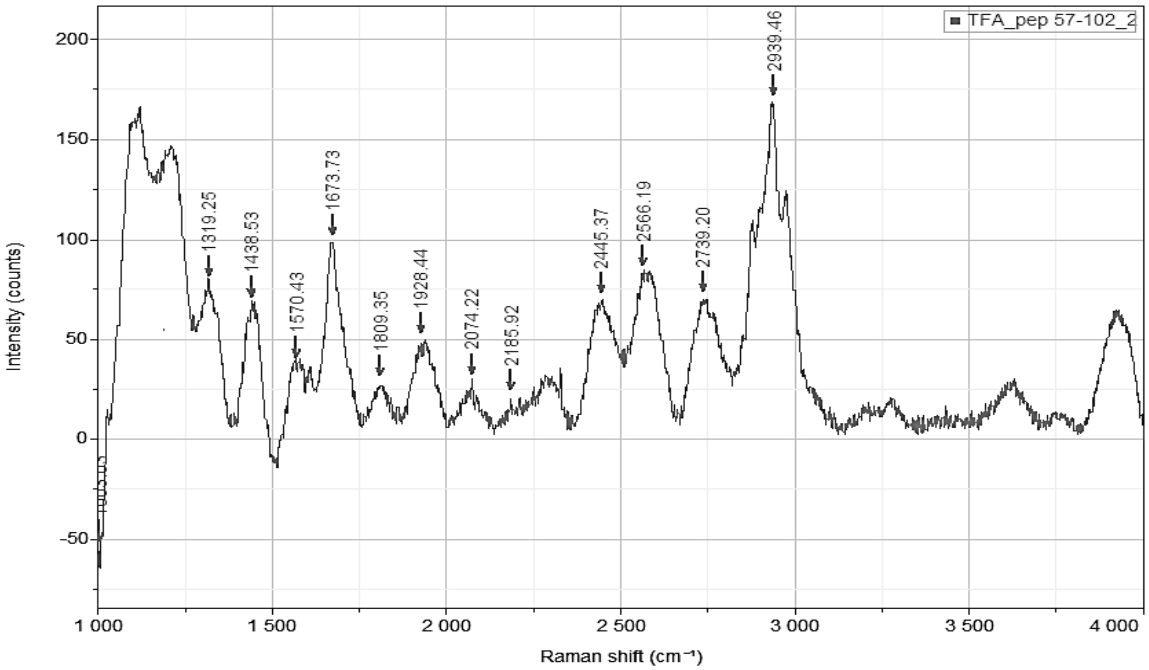

Figure 22. Raman spectrum of purified α-synuclein (57-102) in solid form

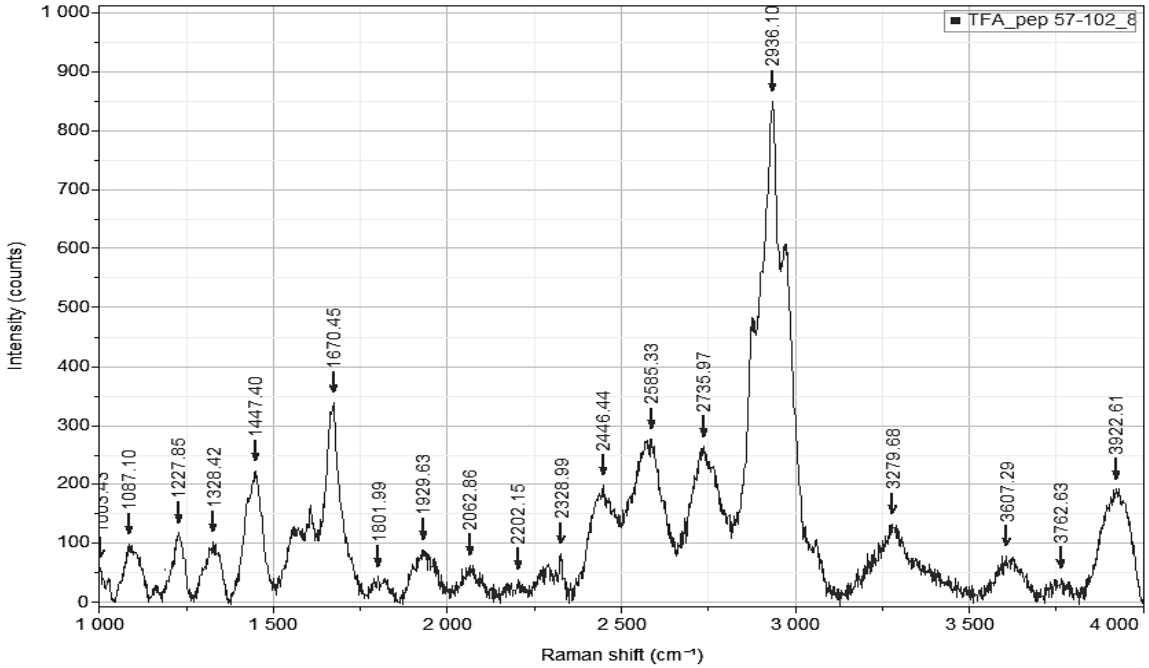

Figure 23. Raman spectrum of purified α-synuclein (57-102) dissolved in DI water

III.V Discussion

As previously mentioned in **Chapter III.I**, α-Synuclein (71-82) had a solubility of 1.48 mg/mL when dissolved in DI water while containing 5 hydrophobic residues and 2 hydrophilic residues. α-Synuclein (66-85) was the least soluble of the three peptides (0.74 mg/mL), but still more soluble than that of the NAC region. This reason may be because it contains 4 hydrophobic residues and only 1 hydrophilic residue. Lastly, α-synuclein (57-102) was the most soluble of the three peptides that were studied (6.25 mg/mL). This increased solubility coincides with the fact that both the N- and C- termini contain more hydrophilic residues, giving the peptide a total of 17 hydrophobic residues in its sequence and doubling the number of hydrophilic residues in its sequence to 11. When comparing α-synuclein (66-85) to α-synuclein (57-102), α-synuclein (61-95) only had a solubility of 0.2 mg/mL when it contained 16 hydrophobic residues and only 5 hydrophilic residues. When doubling the number of hydrophilic residues, as seen in α-synuclein (57-102), the solubility increased to an astounding 6.25 mg/mL. This helps to confirm that adding more hydrophilic residues improves the peptides solubility significantly more than the idea of trying to lower the number of hydrophobic residues (as observed with α-synuclein (71-82)). **Figure 24** helps provide a visual for the solubility of each sample as compared to the solubility of the NAC (α-Synuclein (61-95)) (shown in blue), while also demonstrating the ratio of hydrophobic/hydrophilic residues in a sequence of α-synuclein (shown in red). Each ratio had a direct correlation to its solubility, namely the lower the ratio, the higher the solubility and vice versa.

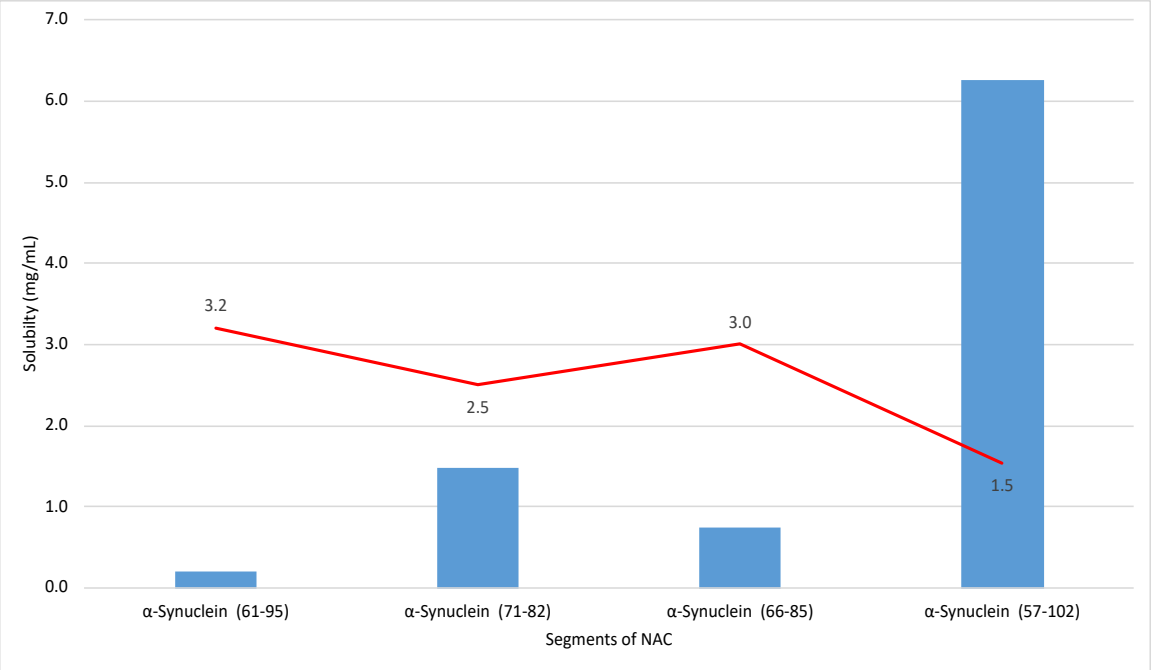

Figure 24. Comparison of solubility of different length NAC segments when dissolved in DI water (Blue); Comparison of ratios of number of hydrophobic residues to hydrophilic residues in different length NAC segments (Red)

When comparing elution percentages, it only took about 24.5-25.5% acetonitrile to elute α-synuclein (71-82), α-synuclein (66-85) took slightly more acetonitrile to elute at 35.4-37.1%. The real difference was for α-synuclein (57-102) which took 83.9-98.6% acetonitrile to elute. It is unclear as to why this peptide eluted so much later than the other two peptides. One speculation is due to how large this peptide was in comparison to the pore size of the column's stationary phase. The peptide may have had difficulty flowing through the column.

It is known that solid Raman may not have biological relevance. The solid Raman can be used as a guide to help determine the secondary structure of the peptide in solution since the solid Raman band peaks have higher intensities and display similar band

peak locations to that of the aqueous Raman, with a few exceptions. When comparing the Raman of the solid state to the peptide dissolved in DI water, it is unclear why the amide III band peaks were significantly different for α-synuclein (71-82) and for α-synuclein (66-85), or why the amide II and C_α–H_b band peaks were significantly different for α-synuclein (57-102). This information still allows us to infer that the solid Raman of the peptides can be used as a guide to predict where the bands of the aqueous Raman will appear once the solubility in solution is increased. Although it is speculation, if one was to assume the structures of the peptides based on this logic and compare the peptide's band peaks to the Raman band peak positions in **Table 2**, one would assume the following.

For α-synuclein (71-82), the amide I band peak fell within the range of a random coil, but the amide II band peak fell within the range of either a random coil or a β-sheet conformation, the amide III band peak did not fall within the ranges for any of the conformations, and the C_α–H_b band peak fell within the range for any of the conformations. The strongest speculation for the secondary structure of α-synuclein (71-82) would be in a random coil conformation in aqueous solution. For α-synuclein (66-85), the amide I band peak fell within the range of either a random coil or a β-sheet conformation. Similar to α-synuclein (71-82), the amide II band peak fell within the range of either a random coil or a β-sheet conformation while the amide III band peak did not fall within the ranges for any of the conformations. The C_α–H_b band peak fell within the range for any of the conformations, concluding the secondary structure for α-synuclein

(66-85) in aqueous solution would be that of a random coil or β-sheet conformation. Lastly, is the discussion of α-synuclein (57-102). The amide I band peak fell within the range of either a random coil or a β-sheet conformation. The amide II band peak did not fall within the ranges for any of the conformations, while the amide III band peak corresponded to that of a β-sheet conformation. Again, the C_α–H_b band peak fell within the range for any of the conformations. It is a stretch to assume, but one could infer that α-synuclein (57-102) would be in a β-sheet conformation in aqueous solution.

CHAPTER IV: CONCLUSIONS & FUTURE PERSPECTIVES

The synthesis and purification of each peptide, α-synuclein (71-82), α-synuclein (66-85), and α-synuclein (57-102), was accomplished. When evaluating the solubility of each peptide, it was concluded that all of them have a better solubility than the NAC region (α-synuclein (61-95)). However, when comparing the solubility of the three peptides, α-synuclein (57-102) overwhelmingly had the best solubility at 6.25 mg/mL. When observing the results for Raman spectroscopy, the band peaks for the solid peptide were in agreement with previously published peak maxima values.[54] Although, the Raman spectroscopy results for the peptides in aqueous solution were nowhere near what we were hoping for, and they definitely need improvement. The main improvement to achieve is to decrease the amount of fluorescence and in turn improve the signal-to-noise ratio. The α-synuclein (57-102) in aqueous solution did seem to show slightly better Raman results than the other two peptides, leading to a deduction that this was due to its increased solubility. The greater the solubility of a peptide in aqueous solution, the more improved the Raman spectroscopy results, leading to greater confidence in the determination of peptide structure.

Optimization is needed to improve the Raman spectroscopy band peaks for peptides in aqueous solution. Due to Raman spectroscopy needing high concentrations for proteins/peptides at around 0.1 mM or above for enough signal for the peaks to be over the noise, other techniques were developed to address this issue.[25] A Raman

technique known as Surface Enhanced Raman Spectroscopy (SERS) was developed that uses metallic nanostructures to enhance the Raman signal by up to $>10^{12}$ orders of magnitude, allowing even single molecule detection. These nanostructures include silver (Ag) and gold (Au), which will be added to a peptide solution in order to observe a signal enhancement of ~10^6 in SERS over Raman spectroscopy.[25] This will be the next step for my lab to improve the Raman spectroscopy data of α-synuclein peptides.

REFERENCES

1. *What Is Parkinson's?*Davis Phinney Foundation. (2017, January 3). https://www.davisphinneyfoundation.org/parkinsons-101/what-is-parkinsons/?gclid=EAIaIQobChMIqbT0qMb16QIV8suGCh2PugPrEAAYBCAAEgKOJfD_BwE (accessed Jun 19, 2020).
2. Marras, C., Beck, J. C., Bower, J. H., Roberts, E., Ritz, B., Ross, G. W., Abbott, R. D., Savica, R., Van Den Eeden, S. K., Willis, A. W., & Tanner, C. M. (n.d.). *Understanding Parkinson's- Statistics*. Parkinson's Foundation. https://www.parkinson.org/Understanding-Parkinsons/Statistics?gclid=EAIaIQobChMI85H3scf16QIV4suGCh3p2gf4EAAYASAAEgI4AvD_BwE (accessed Jun 19, 2020).
3. *Parkinson's 101*. The Michael J. Fox Foundation for Parkinson's Research | Parkinson's Disease. (n.d.). https://www.michaeljfox.org/parkinsons-101 (accessed Jun 19, 2020).
4. *Causes of Parkinson's: American Parkinson Disease Assoc.*APDA. (2019, April 2). https://www.apdaparkinson.org/what-is-parkinsons/causes/?utm_source=google&utm_medium=grants&gclid=EAIaIQobChMI7biOzdP16QIVR9yGCh0skQnNEAAYAiAAEgIqsfD_BwE (accessed Jun 19, 2020).

5. MediLexicon International. (n.d.). *Lewy body dementia and Parkinson's disease*. Medical News Today. https://www.medicalnewstoday.com/articles/lewy-body-parkinsons (accessed Apr 10, 2021).
6. *Parkinson's Disease*. La Jolla Institute for Immunology. (2020, November 19). https://www.lji.org/diseases/parkinsons-disease/ (accessed Apr 10, 2021).
7. Trexler, A. J., & Rhoades, E. Function and Dysfunction of α-Synuclein: Probing Conformational Changes and Aggregation by Single Molecule Fluorescence. *Molecular Neurobiology*, **2012**, *47*(2), 622–631. https://doi.org/10.1007/s12035-012-8338-x (accessed Apr 10, 2021).
8. Lewis, P. A., & Spillane, J. E. Parkinson's Disease. *The Molecular and Clinical Pathology of Neurodegenerative Disease.* **2019**, 83–121.
9. den Hartog Jager, W. A. Sphingomyelin in Lewy Inclusion Bodies in Parkinson's Disease. *Archives of Neurology*. **1969**, *21*(6), 615–619.
10. Mor, D. E., Ugras, S. E., Daniels, M. J., & Ischiropoulos, H. (2015, December 31). *Dynamic structural flexibility of α-synuclein*. Neurobiology of Disease. https://www.sciencedirect.com/science/article/pii/S0969996115301194 (accessed Apr 10, 2021).
11. Eliezer, D., Kutluay, E., Bussell, R., & Browne, G. Conformational properties of α-synuclein in its free and lipid-associated states 1 1Edited by P. E. Wright. *Journal of Molecular Biology.* **2001**, *307*(4), 1061–1073.
12. Stefanis, L. α-Synuclein in Parkinson's Disease. *Cold Spring Harbor Perspectives in Medicine.* **2011**, *2*(2).

13. Bendor, J. T., Logan, T. P., & Edwards, R. H. The Function of α-Synuclein. *Neuron.* **2013**, *79*(6), 1044–1066. https://doi.org/10.1016/j.neuron.2013.09.004 (accessed Apr 10, 2021).
14. YouTube. (2017). *Webinar: "Primary Parkinson's Protein Alpha-synuclein" November 2016*. *YouTube*. https://www.youtube.com/watch?v=eNaWfBTqL5k (accessed Jun 19, 2020).
15. Perez, R. G. Editorial: The Protein Alpha-Synuclein: Its Normal Role (in Neurons) and Its Role in Disease. *Frontiers in Neuroscience.* **2020**, *14*. https://doi.org/10.3389/fnins.2020.00116 (accessed Jul 11, 2021)
16. Waxman, E. A., Mazzulli, J. R., & Giasson, B. I. Characterization of Hydrophobic Residue Requirements for α-Synuclein Fibrillization. *Biochemistry.* **2009**, *48*(40), 9427–9436. https://doi.org/10.1021/bi900539p (accessed Apr 10, 2021).
17. Wang, C., Sharma, S. K., Olaluwoye, O. S., Alrashdi, S. A., Hasegawa, T., & Leblanc, R. M. Conformation change of α-synuclein(61－95) at the air-water interface and quantitative measurement of the tilt angle of the axis of its α-helix by multiple angle incidence resolution spectroscopy. *Colloids and Surfaces B: Biointerfaces.* **2019**, *183*, 110401.
18. Li, S., Combs, J. D., Alharbi, O. E., Kong, J., Wang, C., & Leblanc, R. M. The 13C amide I band is still sensitive to conformation change when the regular amide I band cannot be distinguished at the typical position in H2O. *Chemical*

Communications. **2015**, *51*(63), 12537–12539. https://doi.org/10.1039/c5cc02263k (accessed Apr 10, 2021).

19. Wang, C., Zhao, C., Li, D., Tian, Z., Lai, Y., Diao, J., & Liu, C. Versatile Structures of α-Synuclein. *Frontiers in Molecular Neuroscience.* **2016**, *9*. https://doi.org/10.3389/fnmol.2016.00048 (accessed Apr 10, 2021).
20. Decatur, S. M. Elucidation of Residue-Level Structure and Dynamics of Polypeptides via Isotope-Edited Infrared Spectroscopy. *Accounts of Chemical Research.* **2006**, *39*(3), 169–175.
21. Smith, B. M., & Franzen, S. Single-Pass Attenuated Total Reflection Fourier Transform Infrared Spectroscopy for the Analysis of Proteins in H2O Solution. *Analytical Chemistry.* **2002**, *74*(16), 4076–4080. https://doi.org/10.1021/ac020103v (accessed Apr 10, 2021).
22. Gallagher, W. (n.d.). *FTIR Analysis of Protein Structure*. University of Wisconsin-Eau Claire. https://www.chem.uwec.edu/chem455_s05/pages/manuals/FTIR_of_proteins.pdf (accessed May 3, 2021).
23. Flynn, J. D., Jiang, Z., & Lee, J. C. Segmental 13 C-Labeling and Raman Microspectroscopy of α-Synuclein Amyloid Formation. *Angewandte Chemie International Edition.* **2018**, *57*(52), 17069–17072. https://doi.org/10.1002/anie.201809865 (accessed May 3, 2021).
24. Exline, D. (2019, October 9). *Comparison of Raman and FTIR Spectroscopy: Advantages and Limitations*. Gateway Analytical.

https://www.gatewayanalytical.com/resources/publications/comparison-raman-and-ftir-spectroscopy-advantages-and-limitations/ (accessed Jul. 9, 2021).

25. Devitt, G., Howard, K., Mudher, A., & Mahajan, S. Raman Spectroscopy: An Emerging Tool in Neurodegenerative Disease Research and Diagnosis. *ACS Chemical Neuroscience.* **2018**, *9*(3), 404–420. https://doi.org/10.1021/acschemneuro.7b00413 (accessed Jul. 9, 2021).
26. Oladepo, S. A., Xiong, K., Hong, Z., Asher, S. A., Handen, J., & Lednev, I. K. UV Resonance Raman Investigations of Peptide and Protein Structure and Dynamics. *Chemical Reviews.* **2012**, *112*(5), 2604–2628. https://doi.org/10.1021/cr200198a (accessed May 3, 2021).
27. Sadat, A., & Joye, I. J. Peak Fitting Applied to Fourier Transform Infrared and Raman Spectroscopic Analysis of Proteins. *Applied Sciences.* **2020**, *10*(17), 5918. https://doi.org/10.3390/app10175918 (accessed May 3, 2021).
28. Dehay, B., Bourdenx, M., Gorry, P., Przedborski, S., Vila, M., Hunot, S., Singleton, A., Olanow, C. W., Merchant, K. M., Bezard, E., Petsko, G. A., & Meissner, W. G. Targeting α-synuclein for treatment of Parkinson's disease: mechanistic and therapeutic considerations. *The Lancet. Neurology.* ***2015***, *14*(8), 855–866. https://doi.org/10.1016/S1474-4422(15)00006-X (accessed Jul. 9, 2021).
29. *Fmoc-L-alanine, 99.5% (Chiral HPLC) - Chem-Impex International*. CHEM-Impex. (n.d.). https://www.chemimpex.com/fmoc-l-alanine (accessed May 20, 2021).

30. *Na-Fmoc-Ng-trityl-L-asparagine - Chem-Impex International*. CHEM-Impex. (n.d.). https://www.chemimpex.com/i-n-i-sup-alpha-sup-i-i-fmoc-i-n-i-sup-gamma-sup-trityl-l-asparagine (accessed May 20, 2021).
31. *Na-Fmoc- Nd-trityl-L-glutamine - Chem-Impex International*. CHEM-Impex. (n.d.). https://www.chemimpex.com/i-n-i-sup-alpha-sup-i-i-fmoc-i-n-i-sup-delta-sup-trityl-l-glutamine (accessed May 20, 2021).
32. *Fmoc-L-glutamic acid g-tert-butyl ester hydrate - Chem-Impex International*. CHEM-Impex. (n.d.). https://www.chemimpex.com/fmoc-l-glutamic-acid-gamma-i-tert-i-butyl-ester-hydrate (accessed May 20, 2021).
33. *Fmoc-glycine, 99% (HPLC) - Chem-Impex International*. CHEM-Impex. (n.d.). https://www.chemimpex.com/fmoc-glycine (accessed May 20, 2021).
34. *Fmoc-L-leucine, 99.7% (Chiral HPLC) - Chem-Impex International*. CHEM-Impex. (n.d.). https://www.chemimpex.com/fmoc-l-leucine (accessed May 20, 2021).
35. *Na-Fmoc-Ne-Boc-L-lysine - Chem-Impex International*. CHEM-Impex. (n.d.). https://www.chemimpex.com/i-n-i-sup-alpha-sup-fmoc-i-n-i-sup-epsilon-sup-boc-l-lysine (accessed May 20, 2021).
36. *Fmoc-O-tert-butyl-L-serine, 99.7% (Chiral HPLC) - Chem-Impex International*. CHEM-Impex. (n.d.). https://www.chemimpex.com/fmoc-i-o-i-i-tert-i-butyl-l-serine (accessed May 20, 2021).
37. *Fmoc-L-valine - Chem-Impex International*. CHEM-Impex. (n.d.). https://www.chemimpex.com/fmoc-l-valine (accessed May 20, 2021).

38. *Rink amide MBHA resin (0.3-0.8 meq/g, 200-400 mesh) - Chem-Impex International*. CHEM-Impex. (n.d.). https://www.chemimpex.com/rink-amide-mbha-resin-with-norleucine-br-0-3-0-8-meq-g-200-400-mesh (accessed May 20, 2021).
39. *Fmoc-Asp-OtBu Novabiochem®: Sigma-Aldrich*. Novabiochem®. (n.d.). https://www.sigmaaldrich.com/US/en/product/mm/852037 (accessed May 20, 2021).
40. *Fmoc-Ile-OH Novabiochem®: Sigma-Aldrich*. Novabiochem® . (n.d.). https://www.sigmaaldrich.com/US/en/product/mm/852010 (accessed May 20, 2021).
41. *Fmoc-Phe-OH 4100450 | BACHEM*. BACHEM. (n.d.). https://shop.bachem.com/4100450.html (accessed May 20, 2021).
42. Anaspec. (n.d.). *Fmoc-Thr(tBu)-OH*. Anaspec. https://www.anaspec.com/en/catalog/fmoc-thrtbu-oh~7463ec40-b878-455b-a8f8-5eea93967f3e (accessed May 20, 2021).
43. Anaspec. (n.d.). *1 - Hydroxybenzotriazole hydrate (HOBt hydrate)*. Anaspec. https://www.anaspec.com/en/catalog/1-hydroxybenzotriazole-hydrate-hobt-hydrate~85a0cc6d-2b38-4b1b-a7bb-748490d1fa65 (accessed May 20, 2021).
44. Methylene Chloride (Stabilized/Certified ACS), Fisher Chemical | Fisher Scientific. (n.d.). https://www.fishersci.com/shop/products/methylene-chloride-stabilized-certified-acs-fisher-chemical-7/D37500 (accessed May 20,2021).

45. *Acetonitrile (HPLC), Fisher Chemical | Fisher Scientific*. Fisher Scientific. (n.d.). https://www.fishersci.com/shop/products/acetonitrile-hplc-fisher-chemical-7/A9984#?keyword=Acetonitrile-HPLC%20grade (accessed May 20, 2021).
46. *N,N-Dimethylformamide (Certified ACS), Fisher Chemical | Fisher Scientific*. Fisher Scientific. (n.d.). https://www.fishersci.com/shop/products/n-n-dimethylformamide-certified-acs-fisher-chemical-6/D119500#?keyword=DMF%20(N,N-dimethylformamide) (accessed May 20, 2021).
47. *Ethyl Ether Anhydrous (BHT Stabilized/Certified ACS), Fisher Chemical | Fisher Scientific*. Fisher Scientific. (n.d.). https://www.fishersci.com/shop/products/ethyl-ether-anhydrous-bht-stabilized-certified-acs-fisher-chemical-5/E138500#?keyword=Ethyl%20Ether%20Anhydrous%20(Diethyl%20ether) (accessed May 20, 2021).
48. *Acetic Anhydride (Certified ACS), Fisher Chemical | Fisher Scientific*. Fisher Scientific. (n.d.). https://www.fishersci.com/shop/products/acetic-anhydride-certified-acs-fisher-chemical-4/A10500#?keyword=Acetic%20Anhydride (accessed May 20, 2021).
49. *Piperidine ReagentPlus®, 99%: Sigma-Aldrich*. Sigma-Aldrich. (n.d.). https://www.sigmaaldrich.com/US/en/product/sial/104094?context=product (accessed May 20, 2021).

50. *Triisopropylsilane 98%: Sigma-Aldrich*. Sigma-Aldrich. (n.d.). https://www.sigmaaldrich.com/US/en/product/aldrich/233781?context=product (accessed May 20, 2021).

51. *N,N'-Diisopropylcarbodiimide, 99% - DIC*. Alfa Aesar. (n.d.). https://www.alfa.com/en/catalog/A19292/ (accessed May 20, 2021).

52. *Trifluoroacetic acid, 99% - TFA*. Alfa Aesar. (n.d.). https://www.alfa.com/en/catalog/L06374/ (accessed May 20, 2021).

53. *NI UHP300 - Ultra High Purity Grade Nitrogen, Size 300 High Pressure Steel Cylinder, CGA-580*. Airgas. (n.d.). https://www.airgas.com/p/NI%20UHP300 (accessed May 20, 2021).

54. Kurouski, D., Van Duyne, R. P., & Lednev, I. K. Exploring the structure and formation mechanism of amyloid fibrils by Raman spectroscopy: a review. *The Analyst.* ***2015***, *140*(15), 4967–4980. https://doi.org/10.1039/c5an00342c (accessed Jul. 9, 2021).